TECHNICAL CHALLENGES IN MULTI-MW PROTON LINACS*

V. Lebedev#, FNAL, Batavia, IL 60510, USA

Abstract

The intensity frontier research is an important part of modern elementary particle physics. It uses proton beams to create secondary beams consisting of, but not necessary limited to, neutrinos, muons, kaons and neutrons. Deferent experiments require different time structure of proton beams but all of them require the beam power of about or exceeding 1 MW. In addition, powerful proton linacs can find an application in accelerator driven nuclear reactors and transmutation of radioactive waste. Recent advances in the superconducting RF technology make a multi-MW power level economically acceptable. This paper discusses main physics and technical limitations determining ultimate parameters of such accelerators, their structure and performance.

INTRODUCTION

There are four main applications where MW scale linacs are used or planned to be used. They are: (1) accelerators supporting the intensity frontier research in high energy physics (SPL [1], Project X [2,3], PSI cyclotron [25]), (2) spallation neutron souses (SNS [4], ESS [5], CSNS [6]), (3) accelerators for accelerator driven nuclear power reactors (MYRRA [7], Indian ADS [8], China ADS [9]), and (4) accelerators for nuclear physics (FRIB [10]). Of the aforementioned machines only the SNS is operational. Others are at the design or conception phases. However, all of them use or plan to use superconducting (SC) accelerator cavities. CEBAF commissioned in 1996 [11] is based on the 1 MW recirculating electron linac which is the first MW scale SC linac. Since that time its average accelerating gradient was increased from ~5 to ~7.5 MV/m. The SNS commissioned in 2007 [4] is the first MW scale proton (actually H^-) accelerator. It is based on the experience and technology developed for CEBAF, and presently it is still the only MW scale proton SC linac. Its average accelerating gradient is ~13 MV/m [4]. The recent progress in development of superconducting acceleration cavities is to a large degree based the ILC research [12]. That allowed increasing the accelerating gradient of pulsed machines to well above 30 MV/m. Introduction of SC technology made linacs with MW scale power economically viable and created opportunities which otherwise could not be achieved with normal conducting linac technology.

The proton linacs can be separated into 2 groups: pulsed linacs and continuous wave (CW) linacs. Linacs of the first group are usually used for injection into circular machines and use H^- for the strip injection to the ring. However the ESS will operate in the long pulse regime and accelerate protons. Linacs of the second group usually use protons. However the Project X is based on a CW linac but still uses H^-; a small fraction of those is to be strip-injected into a circular machine for further acceleration. That makes H^- the preferred choice.

A typical layout of a proton linac includes a warm frontend and a main SC accelerator. Normal conducting acceleration for CW machine would result in large power consumption and/or reduced accelerating gradient increasing machine cost. Due to more efficient acceleration the energy of transition from warm to SC part is usually higher for pulsed linacs. Below we will consider main physical and technical limitations for such linacs. For illustration we will be using the SNS, ESS and the Project X. The latter compared to other projects is the most advanced and complicated machine.

The Project-X, a multi-MW proton source, is under development at Fermilab. The Project X configuration is shown in Figure 1. It enables a world-leading program in neutrino physics and a broad suite of rare decay experiments. The facility is based on a 3-GeV 1-mA CW superconducting linac which beam is RF separated to support simultaneous operation of a few experiments [3]. A small fraction of the beam is sent to the 8 GeV pulsed linac operating at 10 Hz repetition rate with about 5% duty cycle. After acceleration to 8 GeV the beam is strip-injected to the Recycler and then sent to the Main Injector for further acceleration. A bunch-by-bunch chopping of CW beam is performed at low energy. It allows one to set a desired time structure for each of 3 GeV experiments and to remove unwanted bunches for the beam directed to a ring. Left untouched these bunches would come to the boundaries of RF buckets and would result in a beam loss.

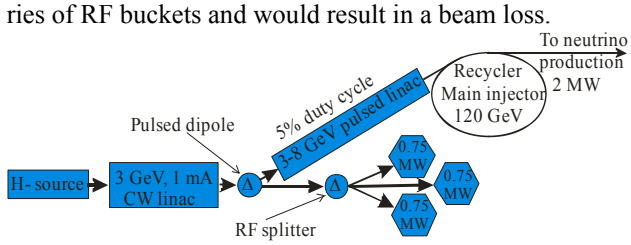

Figure 1: Project X configuration.

WARM FRONTEND LIMITATIONS

A typical scheme of warm frontend is presented in Figure 2. It includes: ion source, low energy beam transport (LEBT), radio-frequency quadrupole accelerator (RFQ), medium energy beam transport (MEBT) and normal conducting part of the linac. The latter is usually not present in CW machines due to high power and low efficiency required for operation.

Presently a machine performance is usually not limited by ion source current or its phase density even in the case of H^- ion source. The volume-cusp ion source developed by TRIUMF [13] is capable of generating a 15-mA DC beam with 0.12 mm mrad normalized rms emittance. The

*Work supported by Fermi Research Alliance, LLC, under Contract No. DE-AC02-07CH11359 with the United States Dep. of Energy
#val@fnal.gov

ISBN 978-3-95450-118-2

SNS H^- pulsed ion source delivers the same beam brightness 125 mA/(mm·mrad) (38 mA, 0.3 mm mrad). The phase density of proton ion sources is higher. In particular, it is more than 3 times higher (450 mA/(mm·mrad)) for the ESS pulsed ion source (90 mA, 0.2 mm mrad) [14]. The ion source life time is a serious issue. It degrades with average current increase and is a more severe problem for H^- sources than for proton souses. For the TRUMPH source the lifetime is only about 350 hours. To mitigate the lifetime problem two ion sources are usually used. One is operating and another is a hot spare which can be live within minutes or even seconds if the primary source dies. The switching from one source to another is performed by a switching dipole.

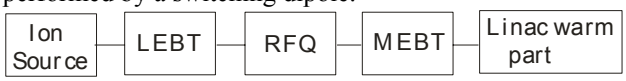

Figure 2: Typical scheme of warm frontend.

The low energy beam transport LEBT section transports the beam to the RFQ and matches the ion source phase space to its entrance. It also serves as a differential pumping section reducing the gas flux from the ion source to the RFQ. The length of LEBT ranges from about 20 cm (SNS) to about 2 m (Project X and ESS). Larger length allows one to make differential pumping more effective and to incorporate an LEBT beam chopper for beam current control in the RFQ. The beam energy in LEBT increases with beam current and usually is in the range from 30 to 80 kV. The beam perveance for most machines is in the range of 60-120 $\mu A/kV^{3/2}$. Two lenses are required to have enough freedom for beam envelope matching. They can be electrostatic einzel lenses (like in SNS) or axially-symmetric magnetic lenses (ESS, Project X). Quadrupoles cannot make the same compact focusing and normally are not used in the LEBT. The beam space charge introduces non-linear focusing which strongly effects single particle motion and results in an emittance growth. For non-relativistic beam its effect is scaled with dimensionless parameter:

$$\kappa_{SC} = \frac{Z_0 I_b L}{4\pi U \varepsilon_n} , \qquad (1)$$

where Z_0=377 Ω, I_b is the peak beam current, eU is the beam energy, ε_n is the normalized beam emittance, and L is distance between focusing elements. For a two-lens transport and $\kappa_{SC} \approx 100$ the space charge increases the beam emittance by ≈ 30%. Note that this growth is also dependent on details of the LEBT optics. To mitigate the emittance growth the space charge compensation by residual gas ions/electrons is used in the case of solenoidal transport which is usually longer and therefore more susceptible to the space charge effects.

RFQ frequency is usually determined by frequency choice of downstream accelerator. For most machines it is 352.2 or 325 MHz – both frequencies suit well the frequency range comfortable for further acceleration. The first choice is bound to the LEP RF frequency allowing one to use infrastructure already existing in CERN; and the second one is bound to the fourth subharmonic of ILC frequency allowing one to use cavity design and experience developed for ILC for acceleration at high energy. The choice of 162.5 MHz for Project X is caused by a requirement of bunch-by-bunch chopping which looks feasible at 162.5 MHz but hardly possible at 325 MHz. Table 1 presents results of a study performed by J. Staples [15] which compares the frequency choices for the Project X RFQ. As one can see the higher frequency RFQ has shorter length (due to faster bunching) and larger power density but other parameters are not much different. Later in the design process the output RFQ energy was reduced to 2.1 MeV to avoid radioactive activation in the RFQ and MEBT. The final parameters and details of the design can be found in Refs. [16, 17]. Space charge effects in the RFQ are important but for presently required beam currents and brightness an acceptable emittance growth can be achieved. In a long run the beam loss results in a degradation of RFQ parameters due to blistering and sputtering. This effect grows proportionally to the beam current loss. Therefore a design of a high power RFQ has to be aimed to minimize the beam loss to the RFQ vanes. In general it is more important for low energy particles which produce more spattering and blistering than high energy particles.

Table 1: Comparison of Project X RFQs Operating at Different Frequencies

	Type 1	Type 2	
Frequency	162.5	325	MHz
Injection Energy	35	30	keV
Output energy	2.5		MeV
Beam current	10		mA
Length	385	287	
Vane-to-vane voltage	98.8	64.2	kV
Peak E-field	20.7	27.6	MV/m
E-field/Kilpatrick	1.52	1.55	
Cavity power	155	149	kW
Max. wall power density	2.1	5.2	W/cm^2
Transmission	94	90	%

The major aim of MEBT is to match the bunch envelopes to the downstream accelerator. In addition to the 2 transverse planes the longitudinal plane has to be matched too. In optimal case it requires at least two RF cavities. As one can see from Eq. (1) an energy increase reduces the space charge parameter but the beam bunching increases the peak current by about an order of magnitude reducing the gain to a factor of 3 to 10 depending on RFQ parameters thus leaving some space for increase of L. That allows one to use quadrupole focusing which results in longer L but is much more effective at a few MeV beam energy. MEBT normally has a diverse set of instrumentation to characterize the RFQ beam, to scrape the beam halo and to assist in the envelope matching. Note that the scraping of longitudinal tails for beam coming out of RFQ is close to impossible. These tails if present will be lost in further acceleration and need to be avoided in a MW scale machine. Therefore one has to pay attention to the longitudinal tails in the course of RFQ design.

Due to bunch-by-bunch chopping the Project X has the

ISBN 978-3-95450-118-2

longest and the most complicated MEBT [18]. The beam envelopes through it are presented in Figure 3. Triplet focusing with ~90 deg. phase advance per cell is chosen. It minimizes the beam sizes and creates "smooth" focusing resulting in relatively small emittance growth. A natural beam divergence results in that a longer kicker requires larger aperture which reduces the kicker effectiveness. To obtain acceptable voltage (power) for the bunch-by-bunch kickers two kickers are used. Each kicker gap is minimized for a given kicker length and beam emittance. To add values of the kicks the kickers are separated by 180 deg in betatron phase. Each kicker [19] has 16 mm gap with 13 mm aperture restriction, 500 mm length, and is driven differentially by two power amplifiers with ±250 V voltage each. Bunches deflected down (see Figure 3) pass the beam absorber and proceed for further acceleration. Bunches deflected up (shown by thick green line in Figure 3) are stopped at the beam absorber. The drift section immediately following the absorber section has a reduced aperture (10 mm) to introduce differential pumping required to prevent performance degradation of the SC cavities due to high gas load from the absorber. The MEBT has three 162.5 MHz normal conducting cavities to prevent beam debunching and to match the longitudinal beam envelope between RFQ and SC linac. The maximum accelerating RF voltage is 100 kV (amplitude). To reduce power density of the chopped beam the beam comes to the beam absorber surface at a grazing angle of 29 mrad. That reduces the power density to acceptable angle but results in that ~25% of particles are coming back from the absorber due to multiple scattering [20]. Molybdenum alloy (TZM) is used as an absorber material. It is resistant to blistering and has a profitable relationship between its thermal conductivity, thermal expansion and the stress yield.

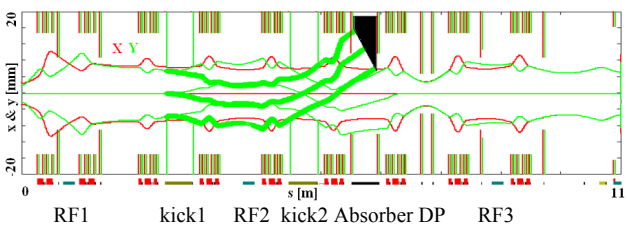

Figure 3: 3σ beam envelopes (ε_{rms_n}=0.25 mm mrad) for accepted and removed bunches through MEBT; red – horizontal plane, green – vertical plane, red and green vertical lines show aperture limitations for *x* and *y* planes.

A usage of SC acceleration at low energy for pulsed machines does not bring significant advantages. Therefore pulsed machines normally use normal conducting accelerating sections between RFQ and SC part of the linac. In particular, the SNS warm part accelerator consists of a Drift Tube Linac (DTL) with 87 MeV output energy, and a coupled-cavity linac (CCL) with 186 MeV output energy. Recent developments in SC cavities reduced the energy where the SC section can start. The ESS plans to use drift tube linac (DTL) to accelerate the beam to 50 MeV. The Project X will be a CW accelerator and its superconducting part starts after MEBT at 2.1 MeV.

SC LINAC LIMITATIONS

The Project X SC linac will accelerate H^- from 2.1 MeV to 8 GeV. Compared to other proposals it uses the largest set of SC cavities and therefore we will use it as a reference for a discussion on design constraints. A layout of the SC part of the Project X is presented in Figure 4. Parameters of cavities and cryomodules are presented in Tables 2 and 3. The acceleration is started by a cryomodule with half-wave resonators (HWR). It continues with two families of single spoke resonators SSR1 and SSR2. Then, at sufficiently high energy it is followed by elliptic resonators. There are two families of 5-cell 650 MHz resonators (LB650 and HB650) assigned for low and high energy acceleration. Finally the acceleration proceeds with ILC type resonators. The status of cavity design and production and other details can be found in Ref. [21].

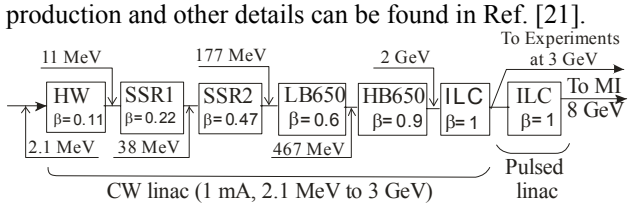

Figure 4: SRF technology map for Project X.

Table 2: Details of SRF Linac Sections

Section	f[MHz]	Cav/mag/CM	L_{CM}[m]	Cell
HWR	162.5	8/8/1	5.83*	S-R
SSR1	325	16/8/2	5.30*	S-R^2
SSR2	325	36/20/4	7.3†	S-R^2
LB650	650	30/10/5	9.5†	D-R^3
HB650	650	96/12/12	13.3†	D-R^8
ILC1(CW)	1300	72/9/9	11.2†	D-R^8
ILC2(pulsed)	1300	224/28/28	11.2†	D-R^8

CM: Cryomodule; D: Doublet, S: Solenoid, R: Resonator, R^n: *n*-number of cavities in one cell. * Length is given together with vacuum valves at both ends. † Preliminary.

Table 3: Parameters of Project X Cavities

Section	β	Aper-ture, mm	Gain MeV	E_{peak} MV/m	B_{peak} mT	R/Q Ohm	G Ohm
HWR	0.11	33	1.8	40	62	225	48
SSR1	0.21	30	2.0	28	70	242	84
SSR2	0.47	40	3.3	32	60	292	109
LE650	0.61	83	11.7	37.5	70	378	191
HE650	0.90	100	17.7	34	61.5	638	255
ILC1	1.0	70	17	34	73	1036	270
ILC2	1.0	70	25	50	107	1036	270

The most challenging beam dynamics problems are at the beginning of SC part of Project X linac. The low bunch repetition frequency of 162.5 MHz required by chopping doubles the single bunch population in compari-

ISBN 978-3-95450-118-2

son with 325 MHz to be used otherwise. Thus with 80% of bunches chopped out and 1 mA average current a single bunch population corresponds to 10 mA; *i. e.* the brightness of the Project X bunches is only ~1.5 times lower than the brightness of SNS beam although average train currents are different in about 40 times. However a usage of 162.5 MHz in the first SC cryomodule mitigates the space charge problem and addresses a few other problems. It significantly improves the beam dynamics due to (1) a larger RF bucket, (2) more linear focusing, (3) a higher accelerating gradient, (4) smaller (closer to on-crest acceleration) accelerating phase; and (5) smaller defocusing due to accelerating RF field. That allowed reducing the number of cavities from 26 SSR0 cavities (operating at 325 MHz and initially planned to be used [3]) to 8 HW cavities. High accelerating gradient in the first cryomodule where energy gain per cavity is comparable to the energy itself creates two problems. The first one is related to longitudinal overfocusing and the second one to transverse defocusing by e.-m. fields of the cavities. The transverse defocusing depends on a particle position in a bunch and therefore it requires stronger focusing from solenoids than one would need for reference particle focusing. These considerations led to the choice that an optical cell of the first cryomodule includes one cavity per solenoid. In spite of that compact focusing structure the accelerating voltage for the first three cavities of the HW cryo-module is reduced so that the longitudinal phase advance would not exceed ~90 degree. For the first cavity the reduction is ~50%.

Both the longitudinal overfocusing and the transverse defocusing decrease with beam energy. That allows reduction in the number of focusing solenoids in the first SSR1 cryomodule where one solenoid follows after two cavities. The relative strengths of space charge effects for both transverse and longitudinal planes are about the same through the beam acceleration. However longitudinal dynamics is additionally affected by the strong non-linearity of the accelerating field focusing; therefore a diligent approach is required for the treatment of longitudinal motion. To reduce the longitudinal motion perturbation at the transition between cryomodules the HW cryomodule is ended with a cavity and the SSR1 cryomodule starts from a cavity. Thus the cryomodules have the following structure: (S-R-S-R-S-R-S-R-S-R-S-R-S-R-S-R) for the HW and (R-S-RR-S-RR-S-RR-S-R) for the SSR1, where R stands for a cavity and S for a solenoid. Using a solenoid as the first element in the HW cryomodule also improves differential pumping between the beam absorber and SC cavities due to cryo-pumping of a cold vacuum chamber located in the solenoid. Its low temperature ($2K^{o}$) results in good cryo-pumping for all gases including hydrogen.

The phase advances per cell at the beginning of HW cryomodule are close to 90^{o} both for transverse and longitudinal planes and decrease to ~30^{o} to the HW cryomodule end. The longitudinal phase advance is larger than the transverse one for first 23 periods ended shortly upstream of the first SSR2 cryomodule end. The beam envelopes and emittance growth for the MEBT and the first 2 cryomodules are shown in Figure 5 [22]. In this section accelerating the beam to ~25 MeV the beam dynamics is space charge dominated in all three planes resulting an emittance growth and halo increase. The emittance growth for both transverse planes is moderate and is within specifications. There is significantly larger growth for the longitudinal emittance mainly related to longitudinal focusing non-linearity but this growth is well within Project X specification. Although the tune depression does not change significantly in the CW linac the emittance growth is comparatively small in the course of further acceleration due to longitudinal tune reduction with acceleration.

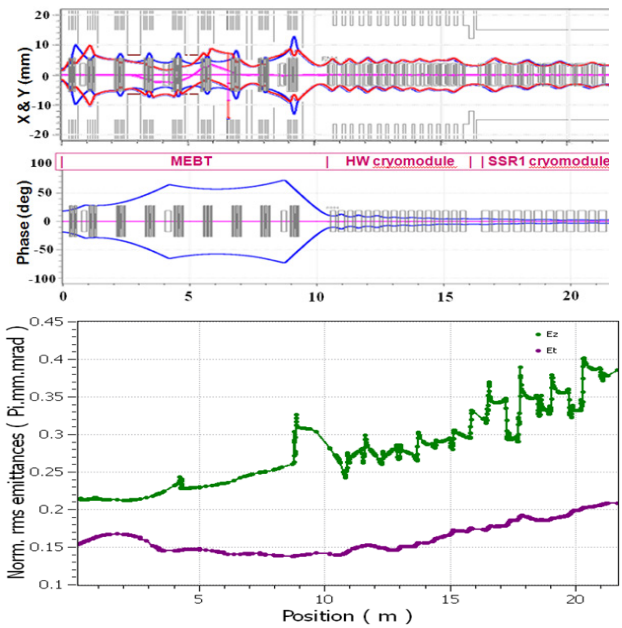

Figure 5: Beam envelopes at 3σ (top) and rms emittances (bottom) for initial part of Project X acceleration; from RFQ to the end of first SSR1 cryomodule; ion source current 5 mA, simulations are performed with TraceWin.

We also studied the implication of a single cavity failure on machine operation. Calculations show that machine operation remains possible with acceptable performance degradation even if the missing cavity is located early in the accelerating path.

BEAM LOSS AND EXTICTION

Achieving low particle loss is the most important requirement for a multi-megawatt machine. The major problems come from the longitudinal particle loss. There are two main reasons. First, in difference to the transverse focusing the longitudinal focusing is non-linear. Second, there is not an acceptable way to scrape the longitudinal tails at the low energy. Due to non-linear potential the motion of particles at large amplitudes is unstable and they are lost in the course of beam acceleration. Both the simulations and the SNS experience show that careful adjustments of accelerating phases in SC cavities allow keeping this loss at an acceptable level. Simulations of the MEBT front end show that if the transverse beam halo is scraped in the MEBT the longitudinal tails are the major

ISBN 978-3-95450-118-2

source of uncontrolled particle losses and that the most losses happens at the designated transverse scrapers installed between cryomodules. In the case of good machine tuning the main source is the long non-Gaussian tails of the RFQ longitudinal distribution which has non-Gaussian tails above 3σ. Simulations also show that particles of very far longitudinal tails are lost extremely fast and cannot be intercepted by scarpers between low energy cryomodules. Such particle slips out of acceleration in the first few cavities and then their energy deviates significantly after passing just one cavity. Finally, overfocusing in a downstream solenoid results in a loss of the particle in the next cavity. Simulations show that even if beam collimators would be installed near each solenoid they cannot intercept major fraction of very far longitudinal tails. Fortunately they also show that the RFQ tails are expected to be sufficiently small and the beam loss at cryogenic surfaces should not exceed few watts.

There is another loss mechanism important in the case of H^- beam. It is the intrabeam stripping (IBST) [23]. Recent experiments carried out in the SNS [24] showed that an increase of H^- beam size due to weaker transverse focusing reduced the beam loss by factor of two and that even in this case the beam loss for H^- beam still is an order of magnitude larger than for the proton beam. Experiments also verified the theory prediction that the radiation excited by the beam loss is distributed comparatively uniformly along the SNS SC linac and that the total particle loss is close to the prediction of $3 \cdot 10^{-5}$. The power loss density in the SNS is estimated to be ~0.15 W/m. It is well within commonly accepted level of 1 W/m required for machine servicing. Calculations performed for the IBST in the Project X result in close values.

Some of Project X experiments may require extremely good extinction for removed bunches. The target value is smaller than 10^{-9}, *i.e.* much less than one particle per bunch. A finite population of longitudinal RFQ tails can be the main limitation to achieve the required extinction. Although there is very good rejection of the tails in the first SC cryomodule the weak longitudinal focusing in MEBT and its large length allow momentum tails of the allowed bunches to move to the nearby rejected bunches and be accepted in their RF bucket. FNAL plans to do an experimental study of the beam extinction at a newly constructed machine named PXIE which will include the first two cryomodules of the Project X and will serve as a prototype for its frontend [22].

DISCUSSION

The limitations described above do not represent fundamental problems to handle a CW beam current up to ~10 mA corresponding to the nominal Project X bunch population. This current corresponds to a 10 MW beam at 1 GeV. Changes to the Project X SRF accelerator required to handle such power are related to upgrade of couplers and RF power and a replacement of 162 MHz RFQ by 325 MHz RFQ. Presently all Project X RF couplers are designed for 5 mA maximum beam current taking into account a possible Project X upgrade to a proton complex of muon collider. The expected beam loss is dominated by IBST and is within specification. Note that for machines which beam is not strip-injected in a ring a proton beam can be used thus decreasing beam loss by about one order of magnitude.

ACKNOWLEDGMENT

The author would like to thank S. Nagaitsev and V. Yakovlev for discussions and help in preparing this manuscript.

REFERENCES

[1] R. Garoby, SRF'2009, p. 930 (2009); http://www.JACoW.org
[2] S. D. Holmes, *et. al*., IPAC'2012, p.3945 (2012); http://www.JACoW.org
[3] "Project X RDR", DocDB-776; http://projectx-docdb.fnal.gov
[4] S. Henderson, PAC'2007, p. 7 (2007); http://www.JACoW.org
[5] H. Danared, IPAC'2012, p. 3904 (2012); http://www.JACoW.org
[6] S. Fu, Linac'10, p. 362 (2010); http://www.JACoW.org
[7] D. Vandeplassche, *et al*., IPAC'2011, p. 2718 (2011); http://www.JACoW.org
[8] P. Singh, SRF'2011, p. 983 (2011);http://www.JACoW.org
[9] S. Fu, Linac'10, p. 437 (2010); http://www.JACoW.org
[10] R. York, PAC'11, p. 2561 (2011); http://www.JACoW.org
[11] A. Hutton, PAC'1997, p. 281 (1997); http://www.JACoW.org
[12] "ILC Reference Design Report"; http://www.linearcollider.org/about/Publications/Reference-Design-Report
[13] http://www.dehnel.com/
[14] R. Miracoli, *et. al*.,"Emittance measurements of intense pulsed proton beam for different pulse length and repetition rate", Rev. Sci. Instrum. **83**, 056109 (2012)
[15] J. W. Staples, "Front-End Issues", Project-X Collaboration Meeting, 11-12 Sep. 2009; http://projectx-docdb.fnal.gov:8080/0002/000278/002/staples.pdf
[16] G.V. Romanov, "IPAC'12, p. 3883 (2012); http://www. JACoW.org
[17] S. P. Virostek, *et. al*.,"IPAC'12, p. 3359 (2012); http://www.JACoW.org
[18] V. A. Lebedev, *et. al.*, "IPAC'12, p. 3874 (2012); http://www.JACoW.org
[19] V. Lebedev, *et al*., "IPAC'12, p. 2708 (2012); http://www.JACoW.org
[20] C. M. Baffes, *et al*., "IPAC'12, p. 2585 (2012); http://www.JACoW.org
[21] V. Yakovlev and C. Ginsburg, "SRF linac technology development", Linac'2012 (2012); http://www.JACoW.org
[22] S. Nagaitsev, *et. al.*, "IPAC'12, p. 3874 (2012); http://www.JACoW.org
[23] V. Lebedev, *et. al.*, Linac'10, p. 929 (2010); http://www.JACoW.org
[24] A. P. Shishlo, *et. al.*, Phys. Rev. Lett. **108**, 114801 (2012).
[25] M. Seidel, et.al., IPAC'2010, p. 1309 (2010); http://www.JACoW.org

ISBN 978-3-95450-118-2